

# Mechanism of Action and Structural Requirements of Constrained Peptide Inhibitors of RGS Proteins

Rebecca A. Roof<sup>1</sup>, Yafei Jin<sup>2</sup>, David L. Roman<sup>1</sup>, Roger K. Sunahara<sup>1</sup>, Masaru Ishii<sup>3</sup>, Henry I. Mosberg<sup>2,\*</sup> and Richard R. Neubig<sup>1</sup>

<sup>1</sup>Department of Pharmacology, 1150 W. Medical Center Dr, University of Michigan, Ann Arbor, MI 48109, USA

<sup>2</sup>Department of Medicinal Chemistry, 428 Church Street, University of Michigan, Ann Arbor, MI 48109, USA

<sup>3</sup>Department of Pharmacology II, Graduate School of Medicine, Osaka University, 2-2 Yamada-oka, Suita, Osaka 565-0871, Japan

\*Corresponding author: Henry I. Mosberg, him@umich.edu

**Regulators of G-protein signaling (RGS) accelerate guanine triphosphate hydrolysis by G $\alpha$ -subunits and profoundly inhibit signaling by G protein-coupled receptors. The distinct expression patterns and pathophysiologic regulation of RGS proteins suggest that inhibitors may have therapeutic potential. We previously reported the design of a constrained peptide inhibitor of RGS4 (1: Ac-Val-Lys-[Cys-Thr-Gly-Ile-Cys]-Glu-NH<sub>2</sub>, S-S) based on the structure of the G $\alpha$ i switch 1 region but its mechanism of action was not established. In the present study, we show that 1 inhibits RGS4 by mimicking and competing for binding with the switch 1 region of G $\alpha$ i and that peptide 1 shows selectivity for RGS4 and RGS8 versus RGS7. Structure-activity relationships of analogs related to 1 are described that illustrate key features for RGS inhibition. Finally, we demonstrate activity of the methylene dithioether-bridged peptide inhibitor, 2, to modulate muscarinic receptor-regulated potassium currents in atrial myocytes. These data support the proposed mechanism of action of peptide RGS inhibitors, demonstrate their action in native cells, and provide a starting point for the design of RGS inhibitor drugs.**

**Key words:** G protein, GTPase activating protein, structure based drug design

**Received 21 February 2006, revised and accepted for publication 12 March 2006**

When activated by an agonist, a G protein-coupled receptor (GPCR) stimulates exchange of guanine triphosphate (GTP) for guanine diphosphate (GDP) on the G $\alpha$ -subunit of the G protein,

which then undergoes an activating conformational change that allows it and its associated  $\beta\gamma$ -subunit to interact with effector proteins (1). The G $\alpha$ -subunit inactivates itself by hydrolyzing GTP to GDP followed by reassociation with G $\beta\gamma$ . Regulators of G-protein signaling (RGS) proteins are GTPase accelerating proteins (GAPs) for G $\alpha$ -subunits (1). They bind to the activated G $\alpha$  protein, stabilize the transition state for GTP hydrolysis without directly interacting with the nucleotide (2), accelerate GTP hydrolysis and inactivation of the G protein, and inhibit cell responses to GPCR signaling.

There are 20 classical RGS proteins and at least 16 RGS homology (RH) domains identified in the human genome (3). The RGS proteins have some G $\alpha$  specificity (1), some receptor specificity (4–7), and unique expression patterns (8–10). Because of this, an RGS inhibitor could selectively potentiate GPCR signaling in specific tissues or brain regions (11,12). Many disease states have been attributed to defects in cell signaling including Parkinson's disease and Alzheimer's disease (13). An RGS inhibitor that could, for example, increase dopamine or acetylcholine responses in specific brain regions may have significant therapeutic potential on its own or might enhance effects of existing agonists in a tissue-specific manner to reduce side-effects (11,12). RGS proteins have also been proposed as therapeutic targets in the treatment of diabetes (14), opioid tolerance (3), heart failure (15), asthma (16), and cancer (17).

The RGS proteins are divided into several families based on the homology of the 120 amino acid RGS domain as well as the presence or absence of other domains (1). Members of the R4 family of RGS proteins are primarily composed of the RGS domain and a short amphipathic N-terminus that plays a role in membrane targeting and/or receptor specificity (18–20). RGS4 is the prototypical member, and the first member of this family for which there was an X-ray crystal structure (21). It also has roles in cardiovascular and central nervous system signaling and was the starting point for our RGS inhibition efforts.

We previously reported the design of a peptide inhibitor of RGS4 (1: Ac-Val-Lys-[Cys-Thr-Gly-Ile-Cys]-Glu-NH<sub>2</sub>, S-S, where S-S indicates disulfide cyclization through the Cys side chain sulfur atoms) based on the structure of the switch 1 region of activated G $\alpha$ <sub>i1</sub> (22). Peptide 1 was designed to bind to RGS in the same way that G $\alpha$ <sub>i1</sub> binds in order to prevent G $\alpha$ /RGS interactions, and, indeed, 1 inhibited RGS4 activity in a membrane-based steady-state GTPase assay with an IC<sub>50</sub> of 26  $\mu$ M (22). Further, 1 has been shown to inhibit RGS4 and RGS8 activity in a capillary electrophoresis pseudo-single turnover GTPase assay (23).

In the present study, we extend these observations to quantify the activity of RGS inhibitor peptides in true single turnover [ $^{32}$ P]GTPase studies with purified G $\alpha$  and RGS proteins. In addition, we examine structure–activity studies to define key features of active peptides, test the mechanism of peptide 1-mediated RGS inhibition by use of the G $\alpha$ ; Gly183Ser mutant, determine the specificity for different RGS proteins, and demonstrate effects of an analog on the kinetics of acetylcholine-stimulated GIRK currents in patch-clamped atrial myocytes.

## Materials and Methods

### Materials

Fmoc-protected amino acids and Rink amide resin were purchased from Advanced ChemTech (Louisville, KY, USA). Preloaded PEG-PS resin, the ABI 431A automated peptide synthesizer, and peptide grade synthesis chemicals were purchased from Applied Biosystems (Foster City, CA, USA).  $\gamma$ -[ $^{32}$ P]GTP (10 mCi/mL) was purchased from Amersham (Piscataway, NJ, USA), or from Perkin-Elmer (Boston, MA, USA) and diluted in unlabeled GTP to the desired level of radioactivity.

### Protein expression and purification

His $_6$ -G $\alpha_o$  (rat), His $_6$ -RGS4 (rat), glutathione S-transferase (GST)-RGS7box (human, nucleotides 915–1359), and GST-RGS8 (rat, nucleotides 315–857) were expressed and purified according to previous protocols (24–26).

### Peptide synthesis

Peptides were synthesized and cyclized as described previously (22). Resin was treated with piperidine (Aldrich, Milwaukee, WI, USA) to cleave the Fmoc-protecting group, then the first amino acid was coupled with *o*-benzotriazol-1-yl-*N,N,N'*-tetramethyl uranium hexafluorophosphate (HBTU) and 1-hydroxybenzotriazole (HOBt; Applied Biosystems). Tri-fluoroacetic acid (TFA)/water/dithioethane (90:5:5) or TFA/phenol/water/triisopropylsilane (88:5:5:2) was used to cleave the linear peptide from the resin and simultaneously remove the side chain-protecting groups. The peptide solution was filtered from the resin and then subjected to preparative reverse-phase high-performance liquid chromatography (RP-HPLC) to afford the linear disulfhydryl-containing peptide with a purity of at least 90%.

### Cyclization of linear peptides

For disulfide formation, linear disulfhydryl-containing peptides were dissolved (1 mg/mL) in 1% acetic acid, 0.1% TFA, 2 M urea in N $_2$  saturated water on ice. The pH of the peptide solution was raised to 8.5 using NH $_4$ OH, followed by the addition of 4 mol equivalents of K $_3$ Fe(CN) $_6$ . The reaction mixture was stirred for 1 min, and quenched with acetic acid to a pH of 3.5 or less. The mixture was then subjected to HPLC.

To form dithioether or dithiomethyl-containing cyclic peptides, a linear disulfhydryl peptide was added to a dimethylformamide solution cooled in an ice bath under a N $_2$  atmosphere (0.1 mg linear peptide/mL dimethylformamide). About 5 mol equivalents of potassium *t*-butoxide were added to the peptide solution, followed by the addition of 2.5 mol equivalents of Br-(CH $_2$ ) $_n$ -Br ( $n = 1$  or 2). The reaction was quenched with 2 mL acetic acid after 2 h and the solvent was removed *in vacuo*. The residue was dissolved in water, filtered, and then subjected to HPLC.

All final product peptides were at least 95% pure as assessed by RP-HPLC on a Vydac 218TP C-18 column (The Nest Group, Southboro, MA, USA) using the solvent system 0.1% TFA in water/0.1% TFA in acetonitrile by a gradient of 0–90% organic component in 90 min. All peptides displayed the appropriate molecular weights as determined by electrospray ionization (ESI) mass spectrometry.

### RGS-stimulated GTPase

Single turnover GTP hydrolysis measurements with and without RGS were based on Lan *et al.* (25) and adapted to a 96-well plate format. Briefly, 200–800 nM G $\alpha_o$  was

loaded with a two- to threefold molar excess of  $\gamma$ -[ $^{32}$ P]GTP in 20 mM HEPES, 20 mM ethylenediaminetetraacetic acid (EDTA) pH 8.0 for 5 or 20 min at room temperature and then cooled on ice. In some cases, the loaded G $\alpha_o$  was gel filtered through a 1 mL G-25 Sephadex spin column to remove unbound [ $^{32}$ P] GTP. The loaded G $\alpha_o$  was then added to equal volumes of ice-cold initiation buffer (20 mM HEPES, 40 mM MgCl $_2$  pH 8.0 and 5–20  $\mu$ M unlabeled GTP) containing RGS and/or peptide $^{11}$ . The concentration of RGS protein (15–500 nM) was varied to keep the uninhibited rate of GTP hydrolysis <5.5 per min. This variation in RGS concentration was needed because of different activities of the protein preparations, different activities of the various RGS proteins against G $\alpha_o$ , and different concentrations of G $\alpha_o$  used. After incubation for various times on ice, the reaction was quenched with 5% activated charcoal in buffer-containing 20 mM sodium phosphate buffer (pH 2.0). After 20 min, the charcoal was centrifuged and the supernatant counted in a Perkin-Elmer TopCount 96-well plate counter by Cerenkov counting. The amount of [ $^{32}$ P]P $_i$  released at each time-point was fit to an exponential function:

$$[^{32}\text{P}]P_i \text{ counts}(t) = \text{counts}_{(t=0)} + \Delta \text{counts}_{(t=30\text{min})} \times (1 - e^{-kt})$$

The rate constant ( $k$ ) was calculated using GraphPad Prism (San Diego, CA, USA). Fitting constraints included setting counts $_{(t=0)}$  for each curve to the average of the counts $_{(t=0)}$  for the experiment, and setting counts $_{(t=30\text{min})}$  to the same value for all curves in an experiment. Peptide activity is determined from the percentage decrease in RGS-stimulated GTPase rate constant ( $k$ ).

### Electrophysiology

All animal studies were performed properly following the guideline of the ethical committee of Osaka University Graduate School of Medicine. Single rat atrial myocytes were enzymatically isolated from hearts removed from adult male Wister–Kyoto rats as described elsewhere (27). Briefly, rats were deeply anesthetized by *i.p.* injection of pentobarbital. A cannula was inserted into the aorta, and the heart was perfused in a retrograde manner through the coronary arteries. The heart was digested by collagenase (Roche Diagnostics, Basle, Switzerland) in nominally Ca $^{2+}$ -free solution at 37 °C for 10 min. Dissociated myocytes were seeded on glass coverslips (15 mm diameter) which had been coated with poly-D-lysine (Sigma, St Louis, MO, USA) kept in a humidified environment of 0.5% CO $_2$  at 37 °C, and cultured with medium M199 (PAA Laboratories, Linz, Austria) containing gentamycin and kanamycin (25 mg/L each) for 2–4 days. Muscarinic receptor-regulated KG channel (GIRK) currents in atrial myocytes were measured using whole-cell mode patch-clamp method as previously described (27). The whole-cell currents were measured at room temperature by a patch-clamp amplifier (Axon 200A, Axon Inst., Sunnyvale, CA, USA) and recorded on videocassette tape with a PCM converter system (VR-10B, Instrutech, Port Washington, NY, USA). Data were analysed with commercially available software (Patch Analyst Pro, MT Corporation, Los Angeles, CA, USA) after low-pass filtering at 1 kHz (–3 dB) by an eightpole Bessel filter, sampled at 5 kHz. The control bathing solution contained (in mM): 115 NaCl, 20 KCl, 1.8 CaCl $_2$ , 0.53 MgCl $_2$ , 5.5 glucose, and 5.5 HEPES-NaOH, pH 7.4. The pipette (internal) solution contained (in mM): 150 KCl, 5 EGTA, 1 MgCl $_2$ , 3 K $_2$ ATP, 0.1 Na $_2$ GTP, and 5 HEPES-KOH (pH 7.3). The ACh-induced GIRK currents were obtained by digitally subtracting currents recorded under control conditions from those recorded in the presence of ACh. Three parameters of RGS action on GIRK currents, *i.e.* time–course of onset ( $k_{on}$ ) and offset ( $k_{off}$ ) of K $_G$  current and degree of relaxation ( $I_{ins}/I_{max}$ ), were determined (27). Peptide 2 was applied intracellularly through the patch capillary electrode. Peptide 2 was first dissolved into dimethylsulfoxide (DMSO) as 15 mM stock, and then diluted at 1/100 into patch electrode internal solution (final internal solution contained 150  $\mu$ M peptides and 1% v/v DMSO).

### Statistical analysis

Data are expressed as mean  $\pm$  SEM and analyzed by either a two-tailed unpaired *t*-test or a one-way ANOVA with a Dunnett's post-test. Significance is indicated as follows: \* $p$  < 0.05, \*\* $p$  < 0.01, \*\*\* $p$  < 0.001.

†Peptides were added from a 5 mM stock in DMSO resulting in a final DMSO concentration of 2% or less which was kept constant for all samples in a given experiment. To avoid precipitation, peptides were never used at concentrations above half of their aqueous solubility limit as determined by HPLC.

## Results

### Peptide 1 inhibits RGS4 GAP activity in a single turnover GTPase assay

We previously showed that **1**, a constrained peptide mimetic of the switch 1 region of  $G\alpha_i$  (Table 1), inhibits RGS4 activity in a steady-state membrane receptor GTPase assay (22). To confirm that **1** is interacting with the RGS4 protein rather than other proteins or lipids in the membrane preparation, we performed single turnover GTPase assays with purified proteins. RGS4-enhanced hydrolysis of  $G\alpha_o$ -bound  $\gamma$ -[ $^{32}$ P]GTP was measured in the presence and absence of **1**. RGS4-stimulated  $G\alpha_o$  GTPase activity is inhibited by **1** in a dose-dependent manner (Figure 1) with an  $IC_{50}$  of  $9 \mu M$ . It should be noted that peptide **1** was tested up to only  $40 \mu M$  (i.e. less than half of its aqueous solubility limit) in order to avoid aggregation. Consistent with our previous results in a membrane GTPase assay (22), the methylene dithioether-bridged peptide **2**, was active but had lower potency than did the disulfide-bridged peptide **1** (Table 1).

### Gly183 is critical for peptide-mediated inhibition of RGS4 GAP activity

It is possible that peptide **1** could bind to either the  $G\alpha$ -subunit or RGS4. In order to determine the target of our peptide inhibitors, peptide **3** was made to mimic the RGS-insensitive Gly183Ser mutant of  $G\alpha_i$ . If peptide **1** binds to RGS4 in the same manner that the switch 1 region of  $G\alpha_i$  binds, then a mutation that disrupts this binding in the  $G\alpha_i$ -subunit should also disrupt binding of peptide **1**. As predicted, peptide **3** does not inhibit RGS4 activity at a concentration that is nearly four times greater than peptide **1** ( $150 \mu M$ ; Figures 2 and 3A), suggesting that **1** binds to RGS4 in a competitive manner with the  $G\alpha$ -subunit. We also prepared peptide **4** using D-Ser in place of the Gly, as D-Ser (unlike L-Ser) is compatible with the  $\beta$ -turn present in the  $G\alpha$  switch 1-RGS4 contact. Interestingly, **4** displayed similar inhibitory properties as **1** in a steady-state GTPase assay (**4**, Table 1 and Figure 3A). A D-Pro analog, **5**, was ineffective at inhibiting RGS4 activation of  $G\alpha_o$ , confirming that the structure of the constrained peptide is important (Table 1 and Figure 3A). This is not surprising as Gly183 is important for  $G\alpha_i$ -RGS4 interactions (25).

### Structure-activity relationship results

In order to better understand which structural components of **1** contribute to its activity, and in hope of identifying more potent inhibitors, several additional modifications to the structure of **1** were examined. The inhibition of RGS4 GAP activity by each peptide at  $100 \mu M$  concentration<sup>†2</sup> was measured using the single turnover GTPase assay and the data are summarized in Table 1. By comparison, **1** inhibits RGS4-stimulated GTPase activity by  $75 \pm 3\%$  at  $40 \mu M$  ( $p = 0.0004$  compared with control).

In compound **1**, incorporation of the N-terminal acetyl and C-terminal carboxamide was chosen to best correspond to the internal 'parent' sequence in  $G\alpha_i$ . In order to examine whether such

electrically neutral termini and the octapeptide framework of **1** are optimal, peptides **6–11** were prepared. As shown in Table 1, analogs with a free N-terminal amine (**6**) or a C-terminal carboxylate (**10**) were inactive (Table 1 and Figure 3B). Truncation of the peptide from either the amino-terminal (**7**) or carboxy-terminal (**11**) end also abolishes activity (Table 1 and Figure 3B). N-terminal elongation of the peptide by either the previous 1 or 3 amino acids in the sequence of  $G\alpha_{i1}$  (compounds **8** and **9**, respectively) also resulted in complete loss of activity (Table 1 and Figure 3B). These suggest that the peptide length and the absence of charged termini are critical for peptide activity.

The Thr182 of  $G\alpha_i$  makes several contacts with RGS4 including interactions with polar (Glu87, Asp163) and non-polar (Leu159) side chains (21). It is therefore not surprising that changing the Thr of **1** to Ala, lacking the polar hydroxyl group, decreases activity (**13**,  $53 \pm 10\%$  inhibition of RGS activity at  $100 \mu M$ , Table 1 and Figure 3C), while the more conservative Ser substitution has intermediate activity (**12**,  $73 \pm 3\%$  inhibition of RGS4 activity at  $100 \mu M$ ; Table 1 and Figure 3C). Substitution of Lys for Thr, with the intention of facilitating a salt bridge with Glu87 of RGS4, was unsuccessful, demonstrating very low inhibitory activity (**14**, Table 1 and Figure 3C).

The structure/conformation of the peptide cycle is also important for activity. In agreement with earlier studies (22), increasing the cycle size from the disulfide of **1** to the methylene dithioether bridge of **2** reduces potency. The latter peptide inhibited RGS4 activity by  $25 \pm 7\%$  at  $100 \mu M$ . Thus, the estimated  $IC_{50}$  for **2** is approximately  $300 \mu M$ , significantly less potent than the disulfide-bonded peptide **1** (Figure 3 and Table 1). Substitution of either disulfide bridge Cys by the more rigid penicillamine (Pen) resulted in complete loss of activity (**15**, **16**; Table 1 and Figure 3C). Substitution of the second Cys with D-Cys also resulted in a complete loss of peptide activity (**17**, Table 1 and Figure 3C). Linear peptides have no activity (22; data not shown).

The Ile184 residue of  $G\alpha_i$  appears to form a van der Waals contact with Tyr84 of RGS4. We found that other hydrophobic residues at this position (**18**, **19**, **20**, **21**) also had some activity (Table 1 and Figure 3C). In particular, peptides with substitution of Met (**18** and **19**) inhibit RGS4 activity by  $22 \pm 9\%$  and  $61 \pm 11\%$  at  $100 \mu M$  (Table 1 and Figure 3C), and Phe (**20** and **21**) inhibits  $38 \pm 10$  and  $52 \pm 12$  at  $100 \mu M$  and  $30 \mu M$ , respectively. Interestingly, the ethylene dithioether-bridged **19** and **21** are more active than the disulfide-bridged **18** and **20**. The opposite is true for the Ile peptides (22).

### Peptides 1 and 2 show RGS specificity

The concentration-dependent effect of **1** on the rate of RGS-stimulated GTP hydrolysis was measured for RGS7 and RGS8 as was carried out for RGS4. The  $IC_{50}$  of **1** on RGS4, RGS7 and RGS8 is  $9 \mu M$ ,  $43 \mu M$  and  $11 \mu M$  respectively (Figure 4A). RGS4 and RGS8 are approximately fourfold more sensitive to **1** than is RGS7. We have previously examined a series of analogs with the same linear sequence as in **1**, but with larger cycles (effected via dithioether

**Table 1:** Sequences and RGS4 inhibition activity of various peptide analogs of **1**

Name	Sequence <sup>a</sup>	Percentage inhibition (100 $\mu$ M unless otherwise noted)
G $\alpha$ (o, i1, i2, and i3)	... <sup>180</sup> Val-Lys-Thr-Thr-Gly-Ile-Val-Glu <sup>187</sup> ...	
<b>1</b>	Ac-Val-Lys-c[Cys-Thr-Gly-Ile-Cys]-GluNH <sub>2</sub> (S-S)	75 $\pm$ 3 (40)
<b>2</b>	Ac-Val-Lys-c[Cys-Thr-Gly-Ile-Cys]-GluNH <sub>2</sub> (S-CH <sub>2</sub> -S)	25 $\pm$ 7
Gly substitutions		
<b>3</b>	Ac-Val-Lys-c[Cys-Thr- <b>Ser</b> -Ile-Cys]-GluNH <sub>2</sub> (S-S)	-10 $\pm$ 8
<b>4</b>	Ac-Val-Lys-c[Cys-Thr-D- <b>Ser</b> -Ile-Cys]-GluNH <sub>2</sub> (S-S)	59 $\pm$ 4 (30)
<b>5</b>	Ac-Val-Lys-c[Cys-Thr-D- <b>Pro</b> -Ile-Cys]-GluNH <sub>2</sub> (S-S)	1 $\pm$ 14
N-terminal modifications		
<b>6</b>	<b>NH</b> <sub>2</sub> -Val-Lys-c[Cys-Thr-Gly-Ile-Cys]-GluNH <sub>2</sub> (S-S)	2 $\pm$ 8
<b>7</b>	Ac-Lys-c[Cys-Thr-Gly-Ile-Cys]-GluNH <sub>2</sub> (S-S)	8 $\pm$ 11
<b>8</b>	<b>Arg</b> -Val-Lys-c[Cys-Thr-Gly-Ile-Cys]-GluNH <sub>2</sub> (S-S)	4 $\pm$ 9
<b>9</b>	<b>Arg-Thr-Arg</b> -Val-Lys-c[Cys-Thr-Gly-Ile-Cys]-GluNH <sub>2</sub> (S-S)	13 $\pm$ 10
C-terminal modifications		
<b>10</b>	Ac-Val-Lys-c[Cys-Thr-Gly-Ile-Cys]-GluOH (S-S)	1 $\pm$ 11
<b>11</b>	Ac-Val-Lys-c[Cys-Thr-Gly-Ile-Cys]-NH <sub>2</sub> (S-S)	3 $\pm$ 29
Thr substitutions		
<b>12</b>	Ac-Val-Lys-c[Cys- <b>Ser</b> -Gly-Ile-Cys]-GluNH <sub>2</sub> (S-S)	73 $\pm$ 3
<b>13</b>	Ac-Val-Lys-c[Cys- <b>Ala</b> -Gly-Ile-Cys]-GluNH <sub>2</sub> (S-S)	53 $\pm$ 10
<b>14</b>	Ac-Val-Lys-c[Cys- <b>Lys</b> -Gly-Ile-Cys]-GluNH <sub>2</sub> (S-S)	19 $\pm$ 15
Cys substitutions		
<b>15</b>	Ac-Val-Lys-c[ <b>Pen</b> -Thr-Gly-Ile-Cys]-GluNH <sub>2</sub> (S-S)	-9 $\pm$ 10
<b>16</b>	Ac-Val-Lys-c[Cys-Thr-Gly-Ile- <b>Pen</b> ]-GluNH <sub>2</sub> (S-S)	-2 $\pm$ 2
<b>17</b>	Ac-Val-Lys-c[Cys-Thr-Gly-Ile-D- <b>Cys</b> ]-GluNH <sub>2</sub> (S-S)	10 $\pm$ 17
Ile substitutions		
<b>18</b>	Ac-Val-Lys-c[Cys-Thr-Gly- <b>Met</b> -Cys]-GluNH <sub>2</sub> (S-S)	22 $\pm$ 9
<b>19</b>	Ac-Val-Lys-c[Cys-Thr-Gly- <b>Met</b> -Cys]-Glu-NH <sub>2</sub> (S-CH <sub>2</sub> CH <sub>2</sub> -S)	61 $\pm$ 11
<b>20</b>	Ac-Val-Lys-c[Cys-Thr-Gly- <b>Phe</b> -Cys]-GluNH <sub>2</sub> (S-S)	38 $\pm$ 10
<b>21</b>	Ac-Val-Lys-c[Cys-Thr-Gly- <b>Phe</b> -Cys]-GluNH <sub>2</sub> (S-CH <sub>2</sub> CH <sub>2</sub> -S)	52 $\pm$ 12 (30)

<sup>a</sup>(S-S), (S-CH<sub>2</sub>-S), (S-CH<sub>2</sub>CH<sub>2</sub>-S), indicate cyclization via disulfide, methylene dithioether, and ethylene dithioether, respectively.

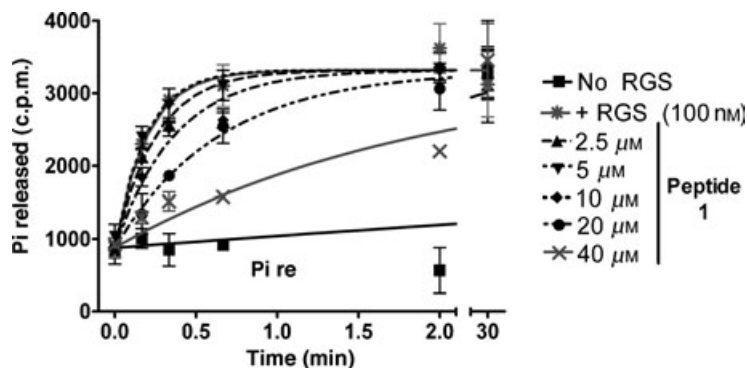


**Figure 1:** Peptide **1** inhibits RGS4 in a single turnover GTPase assay. The rate of guanine triphosphate (GTP) hydrolysis was measured with no regulator of G-proteins signaling (RGS; ■), 100 nM RGS4 (\*), or 100 nM RGS4 with 2.5  $\mu$ M ( $\Delta$ ), 5  $\mu$ M ( $\nabla$ ), 10  $\mu$ M ( $\blacklozenge$ ), 20  $\mu$ M ( $\bullet$ ), or with 40  $\mu$ M ( $\times$ ) **1**. This graph is representative of four experiments carried out in duplicate (mean  $\pm$  SEM).

cyclization). In this series, smaller cycles result in more potent peptide inhibitors of RGS4 (22). The methylene dithioether bridged peptide, **2**, is the second most potent peptide in this series and appears to be selective for RGS4 over RGS8 but has no effect on RGS7 at 100  $\mu$ M (Figure 4B).

**Peptide 2 inhibits RGS regulation of GIRK currents in cardiac myocytes**

To determine whether the peptide inhibitors act in a physiological system and to demonstrate a role of RGS proteins in ion-channel regulation, we used the well-characterized muscarinic GIRK currents

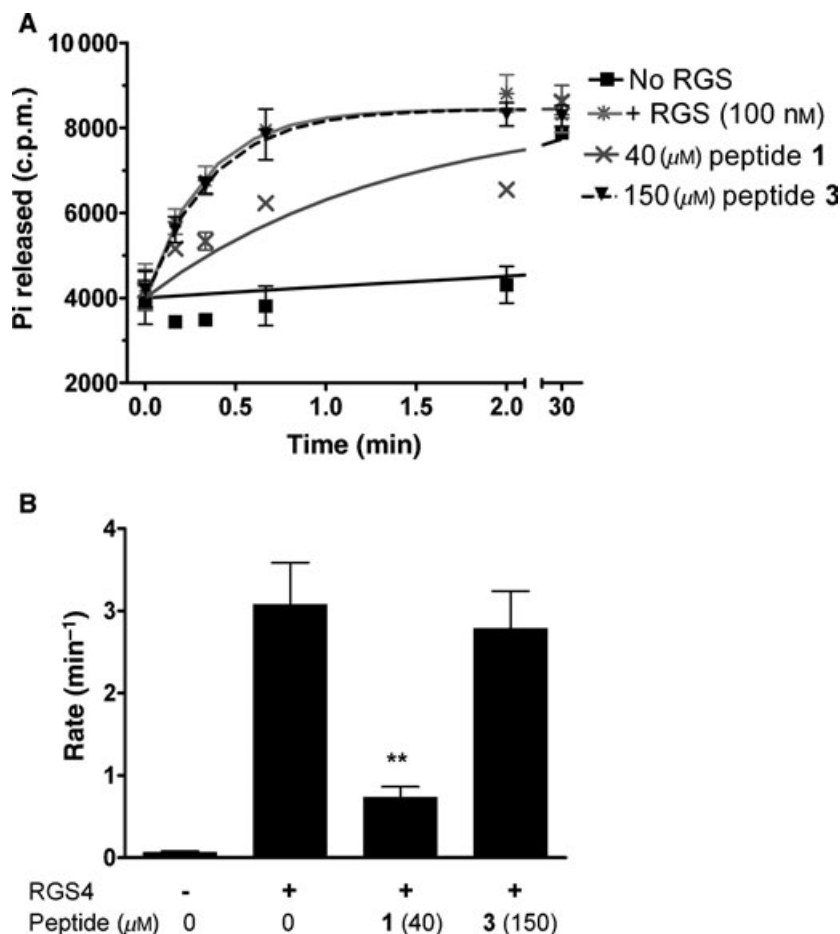


**Figure 2: Gly183 is required for peptide activity at RGS4.** (A) Single turnover GTPase assays were performed as described with no regulator of G-proteins signaling (RGS; ■), 100 nM RGS4 (\*), 100 nM RGS4 with 40 μM **1** (x), and 100 nM RGS4 with 150 μM **3** (▼). This graph is representative of two experiments carried out in duplicate (mean ± SD). (B) Rates were calculated from the data in (A) as described. \**p* < 0.05, \*\**p* < 0.01, \*\*\**p* < 0.001 compared with RGS4 alone.

in atrial myocytes and a whole-cell patch-clamp pipette to deliver the peptides to the intracellular space. The parent peptide **1** had no effect on GIRK currents (not shown), presumably because of residual reducing equivalents in the cell that reduced the essential disulfide bond. The methylene-bridged peptide **2**, however, did reduce the degree of current relaxation (Figure 5A,Ca) and slowed the rate of onset and offset of the muscarinic response (Figure 5B,Cb and d). In some experiments (Figure 5A,Bb) the effect was not seen. Overall, however, there was a statistically significant effect of peptide **2** on all measures of RGS function (Figure 5C).

## Discussion

### Mechanism of action

Peptide **1** was designed based on the crystal structure of the RGS4-Gα<sub>i</sub> complex in the presence of GDPAlF<sub>4</sub>. The peptide attempts to mimic the switch 1 region of Gα<sub>i</sub>, a constrained loop that makes considerable contacts with RGS4. It was designed to bind to RGS4 and competitively inhibit Gα/RGS interactions and thus inhibit RGS4 activity. We showed previously that **1** inhibits RGS4 activity in a steady-state GTPase assay (22) using cell membranes. In the present study, we demonstrated that **1** also inhibits RGS4 activity in a single turnover GTPase assay using purified proteins. The results of these assays unequivocally demonstrate that **1**

is interacting directly with RGS4 protein (or the Gα<sub>o</sub> protein) rather than with other proteins or lipids found in the membrane preparation. Jameson *et al.* recently showed that **1** inhibits both RGS4 and RGS8 in a capillary electrophoresis, pseudo-single turnover GTPase assay (23), also using purified proteins. It was found in that system that **1** had a secondary effect of inhibiting the BODIPY-GTP/Gα<sub>o</sub> interaction; however, that may be an artifact of the BODIPY fluorophore system, as **1** had little direct effect on the rate of GTP hydrolysis by Gα in the γ[<sup>32</sup>P]GTP GAP assays (Figure 4A and Ref 22). From this we conclude that **1** is acting directly on the RGS protein.

To determine whether the mode of interaction of **1** with RGS truly mimics the Gα-subunit interaction, we designed **3** to mimic the switch 1 region of the RGS-insensitive Gly183Ser mutant of Gα<sub>i</sub> (Table 1). The Gly to Ser mutation in the Gα-subunit prevents RGS4 binding (25). We therefore hypothesized that if **1** bound to RGS4 the same way as switch 1 of Gα<sub>i</sub>, then a Gly to Ser modification would prevent peptide inhibition of RGS4 GAP activity. At almost four times the maximal concentration of **1** (150 μM), **3** does not inhibit RGS4 activity (Figure 2), indicating that the Gly in both Gα and in **1** is essential for binding to RGS4. The Gly to Ser modification prevents binding, perhaps due to a direct steric clash of the Ser side chain with RGS4 or through conformational effects on the constrained peptide loop. These data further support the notion that **1** mimics the switch 1 region of Gα to block RGS4 activity on Gα<sub>o</sub>.

Also in support of our proposed mode of action, **1** exhibits significant RGS subtype selectivity. Peptide **1** inhibits RGS4 and RGS8 to a similar extent and inhibits RGS7 less effectively (Figure 4A). RGS4

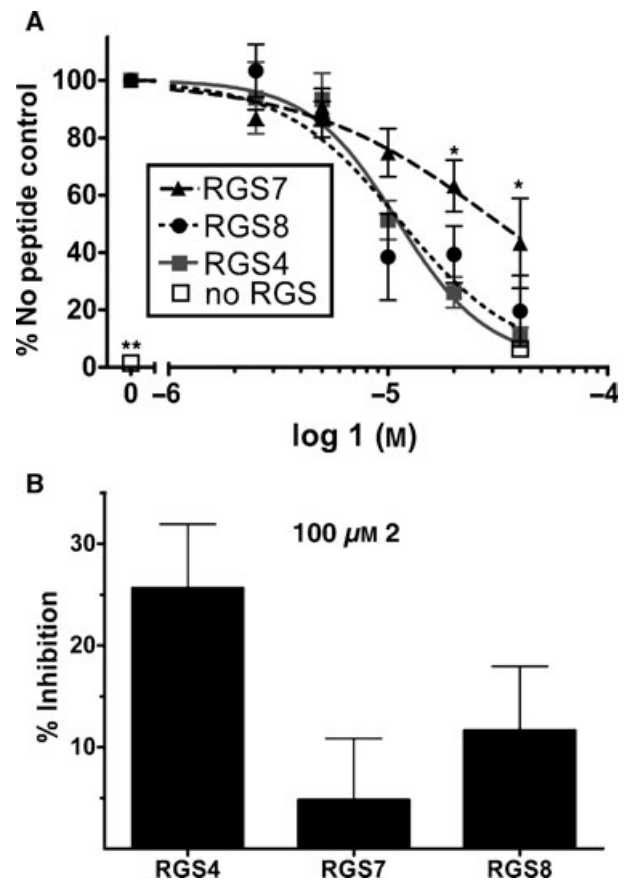
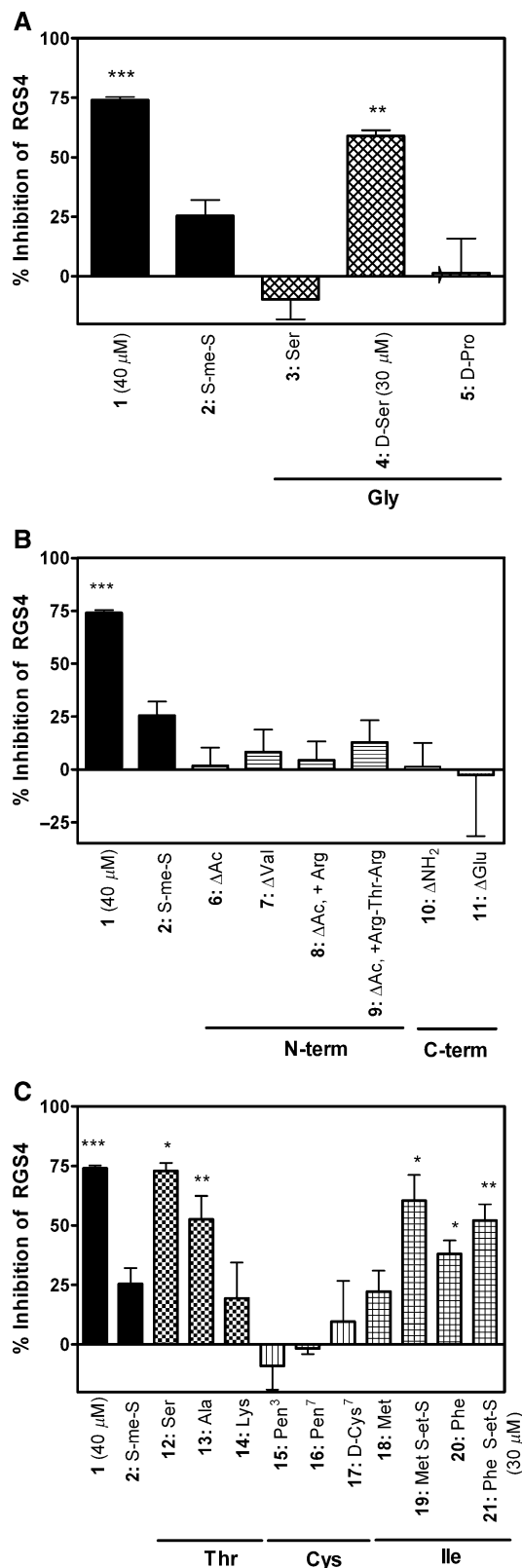


**Figure 4: Peptides 1 and 2 have greater activity for RGS4 and RGS8 than RGS7.** (A) Rate constants were calculated as described in Figure 1, for no regulator of G-proteins signaling (RGS;  $\square$ ), RGS4 ( $\blacksquare$ ), RGS7 ( $\blacktriangle$ ), and RGS8 ( $\bullet$ ) with various concentrations of **1**. These graphs are the average of three (RGS4, no RGS at 40  $\mu$ M **1**), four (RGS7 and RGS8) or five (no RGS, 0  $\mu$ M **1**) experiments carried out in duplicate (mean  $\pm$  SEM). \* $p < 0.05$ , \*\* $p < 0.01$ , \*\*\* $p < 0.001$  compared with RGS4. (B) Percentage inhibition of the rate of RGS4-, RGS7-, and RGS8-stimulated guanine triphosphate (GTP) hydrolysis by 100  $\mu$ M **2** was measured. This is the average of two to eight experiments carried out in triplicate (mean  $\pm$  SEM,  $n = 6-10$ ). \* $p < 0.05$ , \*\* $p < 0.01$ , \*\*\* $p < 0.001$  compared with RGS4.

and RGS8 are both in the R4 family while RGS7 is in the R7 family (11). This family-selective preference of peptide **1** for RGS4 and RGS8 supports our conclusion that it binds to the RGS proteins the same way that  $G\alpha_i$  binds. Further, **1** has little direct effect on the catalytic activity of  $G\alpha_o$  alone (Figure 4 and Ref. 22), from which we conclude that the peptide inhibitor is directly binding to and inhibiting the RGS protein, rather than to the  $G\alpha$  protein. Although

**Figure 3: Inhibition of RGS4 by analogs of 1.** Peptides (from Table 1) were tested in a single turnover GTPase assay at 100  $\mu$ M (unless otherwise indicated) and percentage inhibition of RGS4-stimulated guanine triphosphate (GTP) hydrolysis rate is shown. The modifications from **1** at the indicated position are shown after the peptide number. Inhibition of regulator of G-proteins signaling (RGS) activity by peptides with modifications from **1** at the Gly position (A), at the N- or C-termini (B), or at the Thr, Cys or Ile (C) positions was determined. These graphs are the average of experiments carried out two to four times (mean  $\pm$  SEM,  $n = 2-8$ ). \* $p < 0.05$ , \*\* $p < 0.01$ , \*\*\* $p < 0.001$  compared with RGS4 alone.

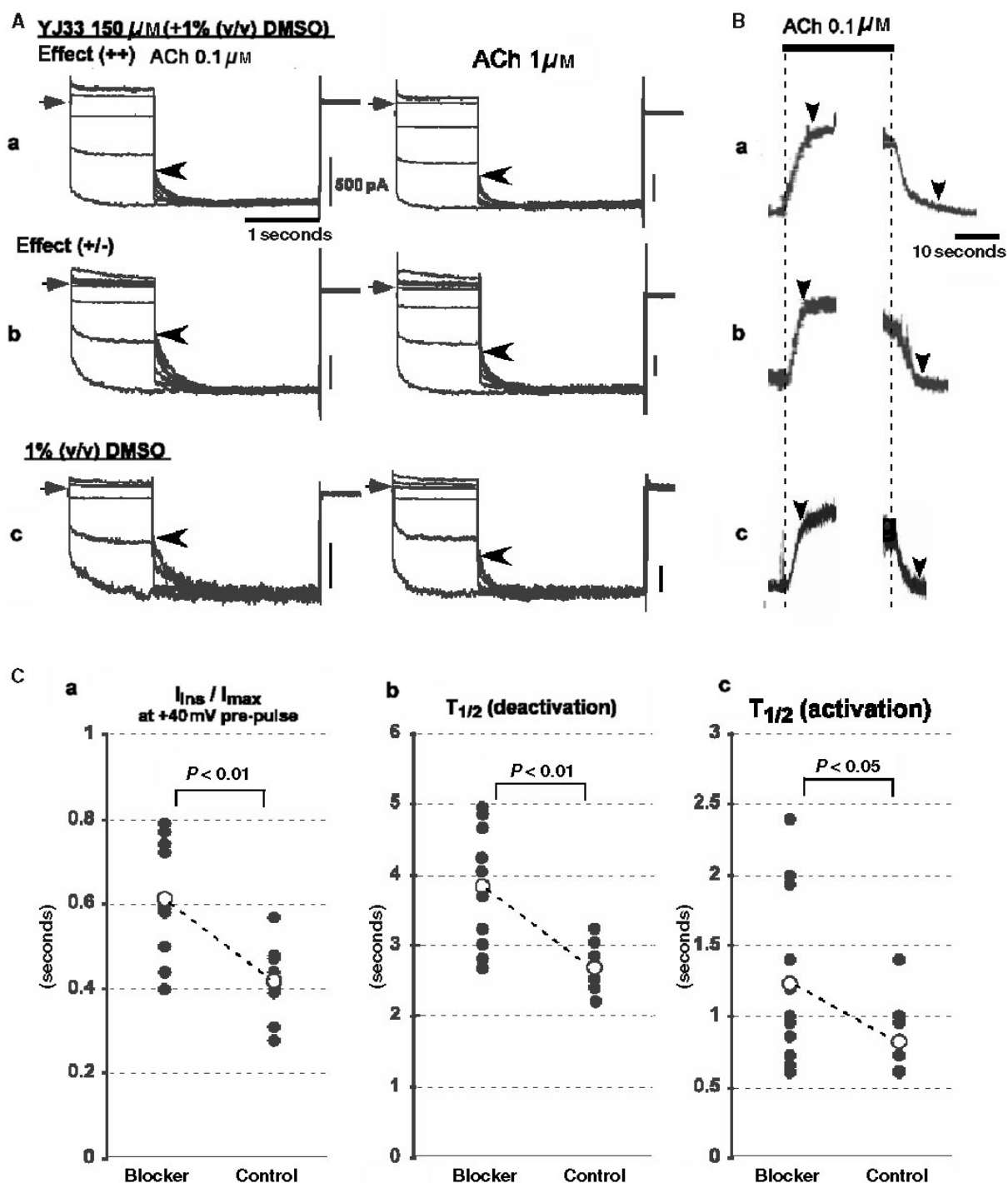


**Figure 5: Inhibition of regulator of G-proteins signaling (RGS) effects on GIRK currents in atrial myocytes by peptide 2.** (A) Representative tracings of currents evoked by 0.1 (left) or 1 (right)  $\mu\text{M}$  acetylcholine in the presence (a and b) or absence (c) of 150  $\mu\text{M}$  **2**, 1% dimethylsulfoxide (DMSO). Sections a and b show the variation of responses to peptide **2**. Currents at  $-100$  mV were recorded after prepulses to  $-100$  to  $+40$  mV in steps of 20 mV. Baseline currents at 0  $\mu\text{M}$  acetylcholine were subtracted out. Arrows indicate the end-point of the instantaneous and the start point of the relaxing components of the currents. Vertical bars represent 500 pA, and horizontal bars indicate 1 second. (B) Representative tracings of deactivation (left) and activation (right) of GIRK currents in the presence (a and b) and absence (c) of 150  $\mu\text{M}$  **2**, 1% DMSO. Sections a and b show the variation of responses to peptide **2**. Arrows indicate the end-point of deactivation or activation and the horizontal bar indicates 10 seconds. (C)  $I_{ns}/I_{max}$ , (a),  $T_{1/2}$  (deactivation; b) and  $T_{1/2}$  (activation; c) were calculated in the presence (left) and absence (right) of 150  $\mu\text{M}$  **2** from (A) and (B) and are shown for individual cells. The mean value is indicated with open circles ( $n = 5-10$  cells).

it is less potent, **2** appears to have similar RGS selectivity and likely shares a similar mechanism of action (Figure 4B).

In the present study, we found peptide **1** to have an  $IC_{50}$  of  $9 \mu M$  against RGS4 (Figure 4A) while in our previous report, in a membrane steady-state GTPase assay, it was less potent with an  $IC_{50}$  of  $26 \pm 2 \mu M$  (22). Peptide **1** inhibited RGS4 81% at  $40 \mu M$  in a capillary electrophoresis assay with  $G\alpha_o$  (23) and is in good agreement with our  $75 \pm 3\%$  inhibition (Table 1). For RGS8,  $40 \mu M$  **1** inhibited 38% and  $74 \pm 23\%$  in the capillary electrophoresis and our single turnover GTPase assays, respectively (23; Figure 4A). Both assays using purified proteins give similar results. However, there are several differences between these systems and the membrane-based steady-state GTPase assay that may contribute to the disparate activities observed. These include the presence of other proteins (including endogenous RGS proteins), various G proteins, the presence of membranes and different temperatures ( $30^\circ C$  in the steady-state assay and ice-cold for the single turnover assay). In addition, the steady-state and the single turnover GTPase assays measure different aspects of the GTP cycle and may thus complicate a direct comparison. The difference is even greater for **2** (Table 1). We show here that RGS4 is inhibited  $24 \pm 5$  per cent at  $100 \mu M$  **2** for an  $IC_{50}$  of about  $300 \mu M$  compared with an  $IC_{50}$  of  $79 \pm 6 \mu M$  in the steady-state GTPase assay (22).

### Structure-activity relationships of peptide inhibitors

Although Val179 and Glu186 of  $G\alpha_i$  do not appear to make direct contacts with RGS4 (21), these residues, with their N- and C-terminal charges blocked, appear to be necessary for peptide activity (Table 1). Perhaps the absence of constraints from the rest of  $G\alpha$  allows these residues and modifiers to make contacts with RGS4 that the switch 1 of  $G\alpha_i$  could not normally make. It is likely that the charges on the free N- or C-termini interfere with binding to RGS4 via adverse electrostatic interactions and the terminal acetyl and amide groups of **1** prevents these negative interactions.

The Thr182 of  $G\alpha_i$  makes contacts with several residues in RGS4 including Glu87 and Asn88 (21). It is therefore not surprising that changing the Thr of **1** to Ala decreases its activity as an RGS4 inhibitor (**13**, Table 1 and Figure 3C), while a more conservative Ser substitution retains considerable activity (**12**, Table 1 and Figure 3C). Glu87 and Asn88 of RGS4 form hydrogen bonds with the hydroxyl group on Thr182 of  $G\alpha_i$  (21). We expect that similar interactions are made with the hydroxyl group of Ser in **12**. We proposed that a Lys in this position might interact with Glu87 on RGS4 and enhance its inhibitory effect; however, the lysine substitution for Thr abolishes activity (**14**, Table 1 and Figure 3C). It is interesting to note that  $G\alpha_{12}$  has a Lys at this position in switch 1, and is not a substrate for RGS4 GAP activity.

Ile184 of  $G\alpha_i$  may form a van der Waals contact with Tyr84 of RGS4. It is therefore not surprising that a peptide with a Met at this position still retains activity as an RGS inhibitor (Table 1 and Figure 3C). It is interesting that **19**, with an ethylene dithioether bridge, is more active than **18** with a disulfide bridge. This is also

the case with Phe substitutions for Ile (**21** and **20**, Table 1 and Figure 3C). The opposite is true for the peptides with the Ile at this position (**22**). Perhaps the alternate conformation of the ethylene bridge positions the Met to make better contact with the RGS4 protein. However, neither peptide is as potent as **1**.

### Peptide RGS inhibitor effects on cardiac GIRK current

This inhibition of RGS-dependent phenomena in atrial myocytes by peptide **2** is the first demonstration of the actions of an RGS inhibitor in a physiologic system. The magnitude of the effect is only modest but is consistent with the  $IC_{50}$  of this peptide at RGS4. The 25% inhibition of *in vitro* single turnover GAP activity seen at  $100 \mu M$  **2** (Figure 4B) and the 25–35% inhibition of  $k_{on}$ ,  $k_{off}$ , and  $I_{ins}/I_{max}$  seen in our patch-clamp studies (Figure 5C) with  $150 \mu M$  **2** are both consistent with a  $K_i$  of about  $300 \mu M$ . The RGS proteins known to be expressed in rat atrial myocytes are 2, 3, 4, 6, 10, 17 (RGSZ2), and 19 (GAIP) (28,29). As GIRK currents are primarily regulated by  $G\alpha_i$ , (30) and RGS 2, 6, and 17, act primarily on  $G\alpha_q$ ,  $G\alpha_o$ , and  $G\alpha_z$ , respectively, RGS 3, 4, 10, and 19 are the best candidates for controlling the kinetics of GIRK currents. Peptide **2** inhibits RGS4 and the sequence similarity of the RGS domain of these other RGS proteins is quite high (43–61%) and greater than that for 7 (35%); it is likely that peptide **2** may inhibit multiple RGS proteins that may be involved in  $G\alpha_i$  and GIRK current regulation.

Here, we show modest specificity of our constrained peptide RGS inhibitors **1** and **2** ( $RGS4 \geq RGS8 > RGS7$ ), provide evidence for the predicted mechanism of the peptide, and show activity in a native cell system. Additional research will clearly be needed to enhance the potency of the peptides, more completely define the RGS specificity, and to develop RGS inhibitors that are cell-permeable for more general use beyond patch-clamp approaches.

### Acknowledgments

The authors would like to thank Katarzyna Sobczyk-Kojiro, Joe Musleh, Eric Schneider, and Liangcai Gu for synthesis of several of the peptides described here. Also would like to thank Irina Pogozheva for help with peptide design, Hailing Zhong for his preliminary work on the project and for preparing the RGS7 and RGS8 proteins, and Emily Jameson for helpful discussions. Authors would like to acknowledge the support of the Michigan Chemistry-Biology Training Program, which is funded through the National Institutes of Health under grant number T32 GM008597. This study was supported by DA03910 and GM39561. This report is dedicated to the memory of our dear friend and colleague, John Omnaas.

### References

1. Hepler J.R. (1999) Emerging roles for RGS proteins in cell signalling. *Trends Pharmacol Sci*;20:376–382.
2. Berman D.M., Kozasa T., Gilman A.G. (1996) The GTPase-activating protein RGS4 stabilizes the transition state for nucleotide hydrolysis. *J Biol Chem*;271:27209–27212.
3. Traynor J.R., Neubig R.R. (2005) Regulators of G protein signaling and drugs of abuse. *Mol Interv*;5:30–41.



4. Wang Q., Liu M., Mullah B., Siderovski D.P., Neubig R.R. (2002) Receptor-selective effects of endogenous RGS3 and RGS5 to regulate mitogen-activated protein kinase activation in rat vascular smooth muscle cells. *J Biol Chem*;277:24949–24958.
5. Xu X, Zeng W., Popov S., Berman D.M, Davignon I., Yu K., Yowe D., Offermann S., Muallem S., Wilkie T.M. (1999) RGS proteins determine signaling specificity of Gq-coupled receptors. *J Biol Chem* 274:3549–3556.
6. Ghavamii A., Hunt R.A., Olsen M.A., Zhang J., Smith D.L., Kalgaonkar S., Rahman Z., Young K.H. (2004) Differential effects of regulator of G protein signaling (RGS) proteins on serotonin 5-HT<sub>1A</sub>, 5-HT<sub>2A</sub>, and dopamine D2 receptor-mediated signaling and adenylyl cyclase activity. *Cell Signal* 16:711–721.
7. Hague C., Bernstein L.S., Ramineni S., Chen Z., Minneman K.P., Hepler J.R. (2005) Selective inhibition of alpha1A-adrenergic receptor signaling by RGS2 association with the receptor third intracellular loop. *J Biol Chem*;280:27289–27295.
8. Kruminis A.M., Barker S.A., Huang C., Sunahara R.K., Yu K., Wilkie T.M., Gold S.J., Mumby S.M. (2004) Differentially regulated expression of endogenous RGS4 and RGS7. *J Biol Chem* 279:2593–2599.
9. Wieland T., Mittmann C. (2003) Regulators of G-protein signalling: multifunctional proteins with impact on signalling in the cardiovascular system. *Pharmacol Ther*;97:95–115.
10. Gold S.J., Ni Y.G., Dohlman H.G., Nestler E.J. (1997) Regulators of G-protein signaling (RGS) proteins: region-specific expression of nine subtypes in rat brain. *J Neurosci*;17:8024–8037.
11. Neubig R.R., Siderovski D.P. (2002) Regulators of G-protein signalling as new central nervous system drug targets. *Nat Rev Drug Discov*;1:187–197.
12. Zhong H., Neubig R.R. (2001) Regulator of G protein signaling proteins: novel multifunctional drug targets. *J Pharmacol Exp Ther*;297:837–845.
13. Standaert D.G., Young A.B. (2001) Treatment of central nervous system degenerative disorders. In: Hardman J.G., Limbird L.E., editors. *Goodman and Gilman's The Pharmacological Basis of Therapeutics*. New York, USA: McGraw Hill; p. 549–568.
14. Usui I., Imamura T., Satoh H., Huang J., Babendure J.L., Hupfeld C.J., Olefsky J.M. (2004) GRK2 is an endogenous protein inhibitor of the insulin signaling pathway for glucose transport stimulation. *EMBO J* 23:2821–2829.
15. Riddle E.L., Schwartzman R.A., Bond M., Insel P.A. (2005) Multi-tasking RGS proteins in the heart: the next therapeutic target? *Circ Res*;96:401–411.
16. Druey K.M. (2003) Regulators of G protein signalling: potential targets for treatment of allergic inflammatory diseases such as asthma. *Expert Opin Ther Targets*;7:475–484.
17. Berman D.M., Wang Y., Liu Z., Dong Q., Burke L.A., Liotta L.A., Fiser R., Wu X. (2004) A functional polymorphism in RGS6 modulates the risk of bladder cancer. *Cancer Res* 64:6820–6826.
18. Hiol A., Davey P.C., Osterhout J.L., Waheed A.A., Fischer E.R., Chen C.K., Millgan G., Druey K.M., Jones T.L. (2003) Palmitoylation regulates regulators of G-protein signaling (RGS) 16 function. I. Mutation of amino-terminal cysteine residues on RGS16 prevents its targeting to lipid rafts and palmitoylation of an internal cysteine residue. *J Biol Chem* 278:19301–19308.
19. Bernstein L.S., Grillo A.A., Loranger S.S., Linder M.E. (2000) RGS4 binds to membranes through an amphipathic alpha-helix. *J Biol Chem*;275:18520–18526.
20. Bernstein L.S., Ramineni S., Hague C., Cladman W., Chidiac P., Levey A.I., Hepler J.R. (2004) RGS2 binds directly and selectively to the M1 muscarinic acetylcholine receptor third intracellular loop to modulate Gq/11alpha signaling. *J Biol Chem* 279:21248–56.
21. Tesmer J.J., Berman D.M., Gilman A.G., Sprang S.R. (1997) Structure of RGS4 bound to AlF<sub>4</sub>-activated G(i alpha1): stabilization of the transition state for GTP hydrolysis. *Cell*;89:251–261.
22. Jin Y., Zhong H., Omnaas J.R., Neubig R.R., Mosberg H.I. (2004) Structure-based design, synthesis, and pharmacologic evaluation of peptide RGS4 inhibitors. *J Pept Res*;63:141–146.
23. Jameson E.E., Roof R.A., Whorton M.R., Mosberg H.I., Sunahara R.K., Neubig R.R., Kennedy R.T. (2005) Real-time detection of basal and stimulated G protein GTPase activity using fluorescent GTP analogues. *J Biol Chem* 280:7712–7719.
24. Lan K.L., Zhong H., Nanamori M., Neubig R.R. (2000) Rapid kinetics of regulator of G-protein signaling (RGS)-mediated Galphai and Galphao deactivation. Galpha specificity of RGS4 AND RGS7. *J Biol Chem*;275:33497–33503.
25. Lan K.L., Sarvazyan N.A., Taussig R., Mackenzie R.G., DiBello P.R., Dohlman H.G., Neubig R.R. (1998) Point mutation in Galphao and Galphail blocks interaction with regulator of G protein signaling proteins. *J Biol Chem* 273:12794–12797.
26. Lee E., Linder M.E., Gilman A.G. (1994) Expression of G-protein alpha subunits in *Escherichia coli*. *Methods Enzymol*;237:146–164.
27. Ishii M., Inanobe A., Fujita S., Makino Y., Hosoya Y., Kurachi Y. (2001) Ca<sup>2+</sup> elevation evoked by membrane depolarization regulates G protein cycle via RGS proteins in the heart. *Circ Res*;89:1045–1050.
28. Doupnik C.A., Xu T., Shinaman J.M. (2001) Profile of RGS expression in single rat atrial myocytes. *Biochim Biophys Acta*;1522:97–107.
29. Kardestuncer T., Wu H., Lim A.L., Neer E.J. (1998) Cardiac myocytes express mRNA for ten RGS proteins: changes in RGS mRNA expression in ventricular myocytes and cultured atria. *FEBS Lett*;438:285–288.
30. Sowell M.O., Ye C., Ricupero D.A., Hansen S., Quinn S.J., Vassilev P.M., Mortensen R.M. (1997) Targeted inactivation of alpha2 or alpha3 disrupts activation of the cardiac muscarinic K<sup>+</sup> channel, IK<sub>ACh</sub>, in intact cells. *Proc Natl Acad Sci U S A* 94:7921–7926.